

teraction. The dimer is stabilized by two two-electron-four-center interactions delocalized over the  $\text{Fe}_2\text{N}_2$  metallacycle and with major contribution from the  $\text{NO } \pi^*_z$  orbitals. The population of the nitrosyl  $\pi^*$  orbitals originates in charge transfer from the  $\pi$  system of the Cp ring to the nitrosyl ligands through the metal atoms. As a consequence, the net charge of each Cp ring becomes positive (+0.25 e). The lability of the Cp  $\pi$  electrons is confirmed by the electron reorganization occurring upon the ionization of the localized metal 3d electrons: the positive hole is shielded by electron transfers originating from the Cp rings and isotropically

directed toward all five metal d orbitals. The net metallic charge in the ionized states therefore remains globally identical with its value in the neutral molecule.

**Acknowledgment.** We thank Prof. Pilloni (University of Padua) for the gift of a sample of the title compound. All quantum-chemical calculations have been carried out on the Cray-1 computer of the CCVR (Palaiseau, France) through a grant of computer time from the Conseil Scientifique du Centre de Calcul Vectoriel pour la Recherche.

Contribution from the Department of Chemistry,  
Princeton University, Princeton, New Jersey 08544

## Electrochemical and Resonance Raman Spectroscopic Characterization of Polyaniline and Polyaniline-Metalloporphyrin Electrode Films

Kathleen A. Macor, Y. Oliver Su,<sup>†</sup> Lisa A. Miller, and Thomas G. Spiro\*

Received January 14, 1987

Characteristics of electropolymerized aniline and metallotetrakis(2-aminophenyl)porphine (metallo-2-TAPP) films are described. Aniline polymerized from methylene chloride solution by oxidative cycling at a platinum electrode shows characteristic two-wave or one-wave cyclic voltammograms when scanned in pH 1 aqueous solution, depending on the positive potential sweep limit. Similar CV's are produced when the solution contains metallo-TAPP's, except that additional waves associated with metalloporphyrin redox processes are superimposed. The absorption spectra of the films formed on transparent  $\text{SnO}_2$  electrodes showed characteristic metalloporphyrin Soret absorption bands, with red shifts relative to the solution spectra, due to axial coordination and/or excitonic effects. Raman spectra are reported for films polymerized from aniline, aniline- $^{15}\text{N}$ , aniline- $N,N$ - $d_2$ , and aniline- $d_5$ . The replacement of strong aniline bands at 1000 and 1029  $\text{cm}^{-1}$  with bands in the films at 1190 and 1200  $\text{cm}^{-1}$  is diagnostic for para-substituted aniline units in the polymer. The films show a strong  $^{15}\text{N}$ -sensitive band at 1525  $\text{cm}^{-1}$ , which is absent in aniline but present in *p*-phenylenediamine. It is assigned to a Fermi resonance between a phenyl ring mode and a combination mode involving an out-of-plane ring motion with substantial N involvement. This band also appears in the TAPP films, superimposed on the strong resonance Raman spectra of the metalloporphyrins. Thus the electrochemical and spectroscopic characteristics of the TAPP films are fully consistent with unmodified porphyrin units contained within a polyaniline polymer. No film formation is observed when a methylene chloride solution of Zn(2-TAPP) is cycled to 0.9 V, just beyond the porphyrin radical cation oxidation wave, but extending the sweep to 1.2 V does lead to polymer formation. Thus, porphyrin radical cation formation is insufficient to induce polymerization if the potential is lower than that required for aniline oxidation. Films containing Mn(2-TAPP) show a  $\text{Mn}^{3+/2+}$  wave at  $\sim -0.2$  V, negative of the polyaniline redox waves, when the electrode is in contact with nonaqueous or aqueous electrolyte. The metalloporphyrin redox process does not require electronic conduction through the polyaniline framework. When polyaniline or polyaniline-porphyrin films are scanned to positive potentials (1.4 V) in contact with aqueous electrolyte, electroactivity is abolished for both the aniline and metalloporphyrin redox waves.

### Introduction

Metalloporphyrins are attractive agents for electrode modification<sup>1</sup> because of their favorable electron transfer characteristics and the possibilities for electrocatalysis associated with the redox reactions of coordinated ligands. Moreover, the strong light absorption in the visible-near-ultraviolet region of the porphyrin  $\pi$  electronic system may prove useful in photoelectrochemical processes.<sup>2</sup> We have previously demonstrated formation of metalloporphyrin electrode films via oxidative electropolymerization of metalloprotoporphyrins from nonaqueous solution.<sup>3</sup> The peripheral vinyl groups of protoporphyrin provide a convenient route for cationic polymerization via the oxidized porphyrin ring. These films showed reversible electroactivity in nonaqueous solvents, but were rapidly inactivated by oxidation when in contact with aqueous solution.<sup>4</sup>

We were attracted to the use of (aminophenyl)porphyrins in electrode film formation because of the known propensity of aniline to form electroactive polymers.<sup>5</sup> During the course of our work Murray and coworkers<sup>6,7</sup> have shown that tetrakis(aminophenyl)porphines do indeed form electroactive polymer films upon oxidative cycling of the electrode potential. Redox processes for the metalloporphyrin units as well as the polyaniline backbone were characterized for a number of systems. Herein we dem-

onstrate via Raman spectroscopy on electrode films that aniline oxidative polymerization proceeds via para substitution, as is commonly supposed, and that electrode films formed by oxidation of tetrakis(2-aminophenyl)porphines (TAPP) contain a polyaniline backbone with pendant and unaltered metalloporphyrin groups. We also show that polymerization requires oxidation of the aniline groups. In contrast to protoporphyrin,<sup>3</sup> (aminophenyl)porphine does not polymerize if only the porphyrin ring is oxidized.

### Experimental Section

*meso*-Tetrakis(2-aminophenyl)porphines (2-TAPP) (Mid-Century Chemicals, Posen, IL) were metalated by refluxing them in DMF with

- (1) (a) Zagal, J.; Sen, R. K.; Yeager, E. J. *J. Electroanal. Chem. Interfacial Electrochem.* **1977**, *83*, 207. (b) Jaeger, C.; Fan, F.; Bard, A. J. *J. Am. Chem. Soc.* **1980**, *102*, 2592. (c) Collman, J. P.; Denisevich, P.; Konai, Y.; Morrocco, M.; Koval, C.; Anson, F. C. *J. Am. Chem. Soc.* **1980**, *102*, 6027. (d) Willman, K. W.; Rocklin, R. D.; Nowak, R.; Kuo, K. N.; Schultz, F. A.; Murray, R. W. *J. Am. Chem. Soc.* **1980**, *102*, 7629. (e) Anson, F. C.; Ni, C.; Saveant, J. M. *J. Am. Chem. Soc.* **1985**, *107*, 3442. (f) Bettelheim, A.; Chan, R. J. H.; Kuwana, T. *J. Electroanal. Chem. Interfacial Electrochem.* **1980**, *110*, 93. (g) Su, Y. O.; Kuwana, T. *Chem. Lett.* **1985**, 459.
- (2) Gouterman, M. In *The Porphyrins*; Dolphin, D., Ed.; Academic: New York, 1978; Vol. 3.
- (3) Macor, K. A.; Spiro, T. G. *J. Am. Chem. Soc.* **1983**, *105*, 5601.
- (4) Macor, K. A.; Spiro, T. G. *J. Electroanal. Chem. Interfacial Electrochem.* **1984**, *163*, 223.
- (5) Chandler, G. K.; Pletcher, D. In *Electrochemistry*; The Royal Chemical Society: London, 1985; Vol. 10.
- (6) White, B. A.; Murray, R. W. *J. Electroanal. Chem. Interfacial Electrochem.* **1985**, *189*, 345.
- (7) Bettelheim, A.; White, B. A.; Raybuck, S. A.; Murray, R. W. *Inorg. Chem.* **1987**, *26*, 1009.

\* To whom correspondence should be addressed.

<sup>†</sup> Present address: Department of Chemistry, National Taiwan University, Taipei, Taiwan, Republic of China.

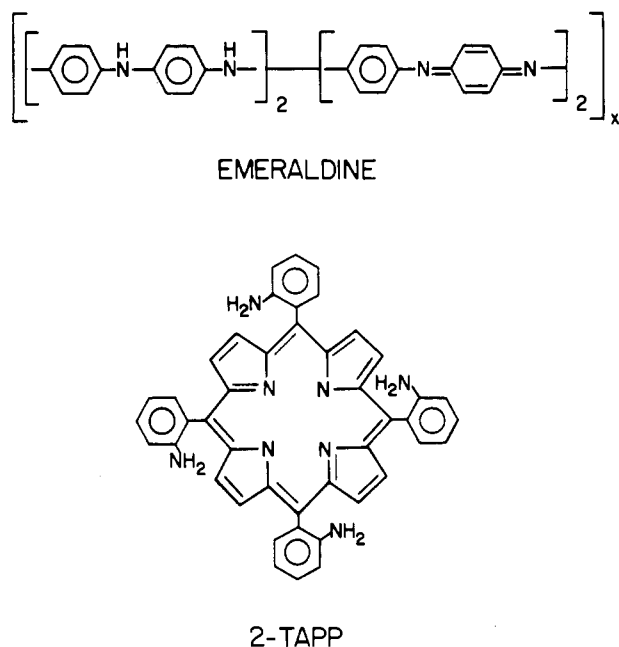


**Figure 1.** Structure of emeraldine and tetrakis(2-aminophenyl)porphine (2-TAPP).

$\text{MX}_2$  salts. The  $\text{M}(2\text{-TAPP})$ 's were purified on alumina columns with  $\text{CH}_2\text{Cl}_2$  as the eluent. Tetrabutylammonium perchlorate (TBAP) (GFS Chemicals, Columbus, OH) was recrystallized twice from ethyl acetate and dried under vacuum. Spectrograde  $\text{CH}_2\text{Cl}_2$  (Mallinckrodt) was used as received. Aniline, aniline- $d_5$  (Aldrich), and aniline- $^{15}\text{N}$  (Stohler Isotope Chemicals, Waltham, MA) were used as received. Aniline- $N,N$ - $d_2$  was prepared by  $\text{CH}_3\text{OD}$  exchange.

Electrochemical experiments were carried out with a Bioanalytical Systems Model CV-27 potentiostat and a Houston Instruments Model 100 X-Y recorder. A saturated calomel electrode (SCE) was used as the reference electrode. Platinum foil (Alfa) was used for the working electrodes. Electronic spectra of films on optically transparent  $\text{SnO}_2$  electrodes (PPG Industries, Pittsburgh, PA) were obtained with a Hewlett-Packard Model 8450 spectrophotometer.

Exciting radiation for resonance Raman spectra was provided by Coherent Radiation CR-5  $\text{Ar}^+$  (4880 Å) and Spectra Physics 171  $\text{Kr}^+$  (4131, 4067 Å) lasers. The scattered radiation was dispersed by a Spex 1401 double monochromator and detected by a cooled RCA 31034A photomultiplier tube by using an Ortec 9315 photoncounting system, under the control of a MINC (DEC) minicomputer. Spectra were recorded digitally by backscattering off of the electrodes, which were rotated to prevent laser-induced sample damage.<sup>8</sup>

## Results and Discussion

**A. Polyaniline.** Polymers formed by oxidizing aniline have been studied extensively,<sup>9-11</sup> but structural characterization has been sparse. Many possible polymer structures have been proposed: (a)  $p\text{-C}=\text{N}$  bond formation resulting from "head-to-tail" polymerization,<sup>9</sup> (b)  $m\text{-C}=\text{N}$  bond formation,<sup>12</sup> (c)  $\text{N}=\text{N}$  linkages from "head-to-head" reactions<sup>12</sup> and (d)  $\text{C}-\text{C}$  benzidine species from "tail-to-tail" polymerization.<sup>13</sup> Possible products of aniline oxidation include emeraldine and negraniline (Figure 1), eight-ring species resulting from "head-to-tail" polymerization.<sup>14</sup> An early study of the anodic precipitate from electrochemical oxidation of acidic aniline solutions suggested the presence of emeraldine units on the basis of infrared and chemical tests.<sup>15</sup>

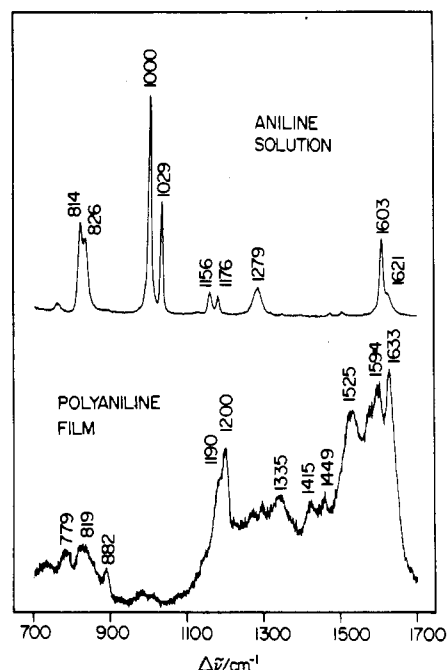


**Figure 2.** Resonance Raman spectra of aniline solution and polyaniline film with 4880-Å excitation and 6- $\text{cm}^{-1}$  slit widths.

Current interest in polyaniline films centers on their metallic conductivity when they are formed from acidic solution. Infrared studies of such films suggest that they are very similar to emeraldine, possibly with a small amount of benzidine subunits.<sup>10,12</sup> Polyaniline films formed from basic solution are insulators and have been suggested, on the basis of infrared spectra, to contain meta-polymer products.<sup>12</sup> On the other hand soaking these insulating films in acid restores electrode conductivity;<sup>11</sup> it seems unlikely that acid soaking could lead to a change in the substitution pattern of the polymer. For polyaniline films formed in acetonitrile/pyridine solutions both para- and meta-substituted ring structures have been reported, based on the infrared spectral pattern in the  $\text{C}-\text{N}$  stretching region or in the 700-900- $\text{cm}^{-1}$  fingerprint region.<sup>16</sup> Structural inferences from infrared spectroscopy are not very secure for these species because of the richness of the spectra; the studies cited have not used isotopic substitution to aid in spectral assignments.

We believe Raman spectroscopy to provide more definitive structural characterization because of the characteristic dependence of the Raman spectral pattern on the disposition of the ring substituents of aromatic compounds.<sup>17</sup> Figure 2 compares the Raman spectrum of aniline in solution with that of a polyaniline film electropolymerized from  $\text{CH}_2\text{Cl}_2$  on a Pt electrode (dried, in air). At the laser wavelength used, 488.0 nm, the polyaniline film may well be subject to resonance enhancement; it has a broad unstructured absorption throughout the visible region.<sup>9</sup> Consequently, relative intensity differences between the two spectra may reflect resonance effects primarily. Nevertheless it is striking that the strongest aniline bands, at 1000 and 1029  $\text{cm}^{-1}$ , are completely absent in the polyaniline spectrum. These ring modes ( $\nu_{12}$  and  $\nu_{18a}$ ) are characteristic of monosubstituted benzenes.<sup>17</sup> For disubstituted benzenes, the 1000- $\text{cm}^{-1}$  band remains when the substitution is meta while a band near 1029  $\text{cm}^{-1}$  ( $\nu_{18b}$ ) remains when the substitution is ortho. Para-disubstituted benzenes show neither band but show strong intensity for ring mode  $\nu_{9a}$ , near 1200  $\text{cm}^{-1}$ , and a nearby band, which has mixed ring and ring-substituent stretching character.<sup>17</sup> This is precisely the pattern seen

(8) Czernuszewicz, R. S. *Appl. Spectrosc.* **1986**, *40*, 571.

(9) Diaz, A. F.; Logan, J. A. *J. Electroanal. Chem. Interfacial Electrochem.* **1980**, *111*, 111.

(10) Kobayashi, T.; Yoneyama, H.; Tamura, H. *J. Electroanal. Chem. Interfacial Electrochem.* **1984**, *161*, 419.

(11) Huang, W. S.; Humphrey, B. D.; MacDiarmid, A. G. *J. Chem. Soc., Faraday Trans. 1*, **1986**, *82*, 2385.

(12) Ohsaka, T.; Ohnuki, Y.; Oyama, N.; Katagiri, G.; Kamisako, K. *J. Electroanal. Chem. Interfacial Electrochem.* **1984**, *161*, 399.

(13) Bacon, J.; Adams, R. N. *J. Am. Chem. Soc.* **1968**, *90*, 6596.

(14) Green, A. G.; Woodhead, A. E. *J. Chem. Soc.* **1910**, *97*, 2388; **1912**, *101*, 117.

(15) Mohilner, D. M.; Adams, R. N.; Argersinger, P. *J. Am. Chem. Soc.* **1962**, *84*, 3618.

(16) Volkov, A.; Tourillon, G.; Lacaze, P. C.; Dubois, J. E. *J. Electroanal. Chem. Interfacial Electrochem.* **1980**, *115*, 279.

(17) Dollish, F. A.; Fateley, W. G.; Bentley, F. F. *Characteristic Raman Frequencies of Organic Compounds*; Wiley-Interscience: New York, 1974; Chapter 13.

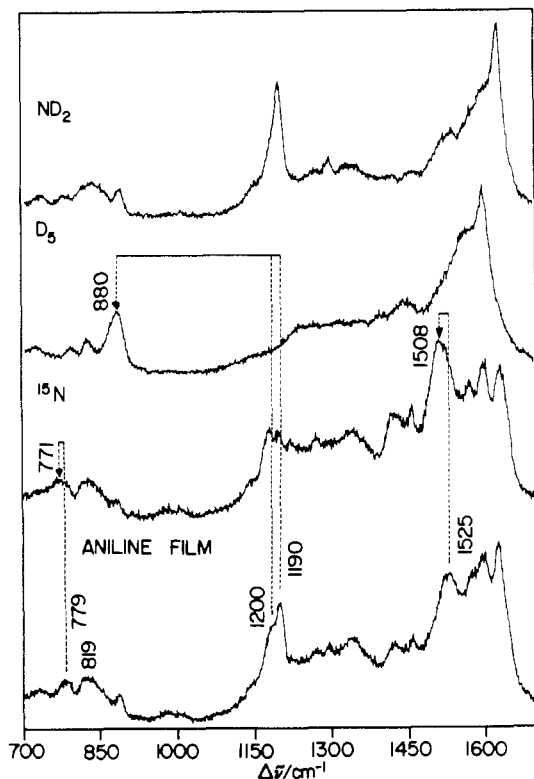


**Figure 3.** Resonance Raman spectra of polyaniline film and polyaniline films prepared with aniline- $^{15}\text{N}$ , aniline- $d_5$ , and aniline- $N,N-d_2$ . Laser excitation was 4880 Å and slit widths were 6  $\text{cm}^{-1}$ .

in the polyaniline film spectrum: no bands at 1000 or 1029  $\text{cm}^{-1}$  but a strong doublet at 1190 and 1200  $\text{cm}^{-1}$ . Thus the film Raman spectrum provides clear-cut evidence for para substitution in the polymer; the fraction of ortho or meta substitution must be very small.

To examine further the nature of the film Raman spectrum we prepared films with isotopic substitution, using aniline- $d_5$ , aniline- $^{15}\text{N}$ , and aniline- $N,N-d_2$ . Their Raman spectra are compared in Figure 3. The most interesting result is that the strong 1525- $\text{cm}^{-1}$  polyaniline band shifts down 17  $\text{cm}^{-1}$  upon  $^{15}\text{N}$  substitution. No band is seen at this frequency for aniline, but *p*-phenylenediamine does have a Raman band at 1522  $\text{cm}^{-1}$ .<sup>18</sup> This has been assigned<sup>18</sup> to the result of a Fermi resonance interaction between a ring mode near 1600  $\text{cm}^{-1}$  and a combination of the 820- $\text{cm}^{-1}$  CH bending mode and an out-of-plane ring deformation mode at 730  $\text{cm}^{-1}$ . A similar assignment is likely for polyaniline, which shows several ring modes in the 1600- $\text{cm}^{-1}$  region. The Fermi resonant combination mode could be built on the 819- and 779- $\text{cm}^{-1}$  frequencies. We note that the 779- $\text{cm}^{-1}$  band shifts down by  $\sim 8$   $\text{cm}^{-1}$  upon  $^{15}\text{N}$  substitution, perhaps reflecting N involvement in the out-of-plane deformation. In any event, the existence of 1525- $\text{cm}^{-1}$  Raman bands for both *p*-phenylenediamine and polyaniline strengthens the inference that the substitution pattern in the polymer is para.

We note that a polyaniline infrared band at 1620  $\text{cm}^{-1}$  has been assigned to C=N stretching.<sup>16</sup> There is a Raman band at 1633  $\text{cm}^{-1}$ , but it shows no shift upon  $^{15}\text{N}$  substitution (Figure 3) and it is assigned instead to a ring mode. We do not observe any  $^{15}\text{N}$ -sensitive band in the C=N stretching region, as might be anticipated from the structure of emeraldine. The Raman spectra were obtained, however, on film that may well have been largely reduced when the electrode circuit was opened.  $^{15}\text{N}$  sensitivity is evident in the  $\sim 1200$ - $\text{cm}^{-1}$  region, where C=N stretching contributions are expected, but the band structure is complex and the shifts are not easy to determine. It will be of interest to monitor the Raman spectrum of polyaniline film in situ as a function of

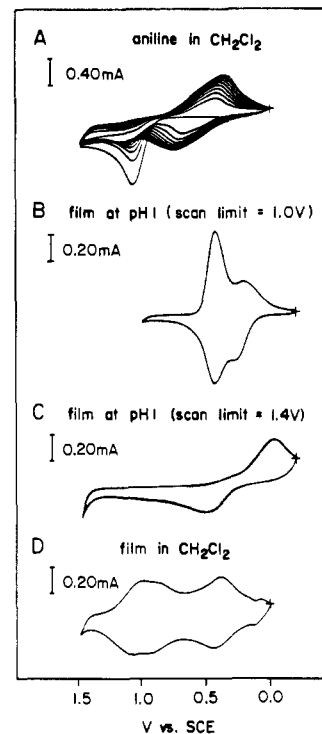


**Figure 4.** Cyclic voltammograms: (A) aniline in  $\text{CH}_2\text{Cl}_2$ ; (B and C) polyaniline film in pH 1 solution; (D) polyaniline film in  $\text{CH}_2\text{Cl}_2$ . Scan rate was 100 mV/s.

electrode potential; substantial changes upon progressive film oxidation are anticipated.

Large spectral changes are seen for film prepared with aniline- $d_5$ , because of the involvement of CH bending in the ring modes.<sup>19</sup> This involvement is particularly large for the modes near 1200  $\text{cm}^{-1}$ ; the characteristic 1190/1200- $\text{cm}^{-1}$  doublet is eliminated in the aniline- $d_5$  film and the intensity is shifted to the 880- $\text{cm}^{-1}$  band. The  $\sim 1600$ - $\text{cm}^{-1}$  ring modes are also perturbed, and the 1525- $\text{cm}^{-1}$  band has lost most of its intensity, consistent with perturbation of the proposed Fermi resonance. Much of the 1525- $\text{cm}^{-1}$  band intensity is also lost in the aniline- $N,N-d_2$  film, suggesting some involvement of ND bending. The intensity distribution in the 1190/1200- $\text{cm}^{-1}$  doublet is also altered (as it is in the  $^{15}\text{N}$ -substituted film) due to the involvement of ring-substituent (NH) stretching in these modes.

These polyaniline films, prepared by positive potential cycling of electrodes in  $\text{CH}_2\text{Cl}_2$  solutions of aniline, are electroactive, as shown in Figure 4. The initial sweep for a  $\text{CH}_2\text{Cl}_2$  aniline solution shows an aniline oxidation wave at 1.06 V, which is progressively replaced by polymer waves at lower potential. When the electrode with the polyaniline film is placed in pH 1 aqueous solution, a CV is obtained with two dominant waves at 0.2 and 0.4 V. This pattern has been observed by other workers, and Bacon and Adams<sup>13</sup> postulated that the two redox couples are associated with *N*-phenyl-*p*-phenylenediamine and benzidine units in the polymer. These overlapping waves account for the electronic conductivity of the film between  $\sim 0$  and +0.6 V. We can actually detect four redox couples at 0.1, 0.4, 0.9, and 1.0 V in TBAP/methylene chloride, no doubt reflecting significant interactions among the various redox sites in the polymer.

On the other hand, other workers have reported seeing only a single broad redox wave for polyaniline in aqueous solution with  $E_{1/2} \sim 0.3$  V.<sup>9</sup> We have been able to reproduce this behavior as well (Figure 4) by cycling the potential to more positive values, 1.4 V. Thus the nature of the polymer is affected by the potential limit used in oxidizing the aniline. The films must nevertheless be structurally very similar in the two cases, since RR spectroscopy

(18) Ernstbrunner, E. E.; Girling, R. B.; Grossman, W. L.; Mayer, E.; Williams, K. J.; Hester, R. E. *J. Raman Spectrosc.* **1981**, *10*, 161.

(19) (a) Scherer, J. R. *Planar Vibrations of Chlorinated Benzenes*; Dow Chemical Co.: Midland, MI, 1963. (b) Scherer, J. R. *Spectrochim. Acta, Part A* **1968**, *24A*, 747.

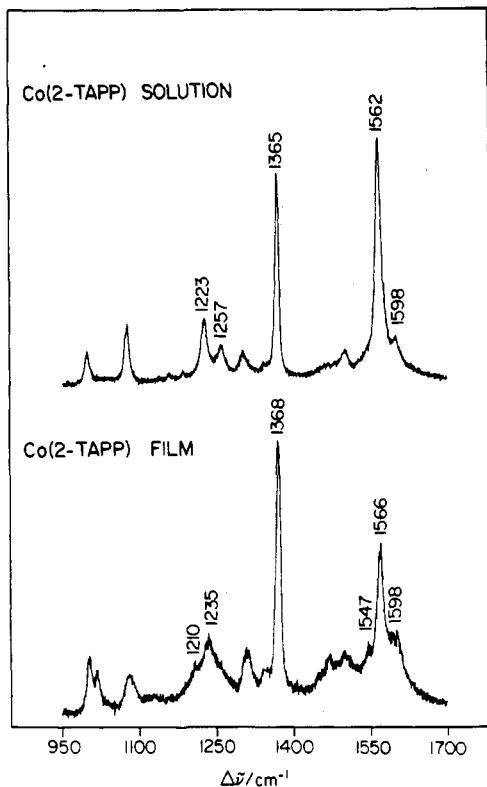


**Figure 5.** Resonance Raman spectra of Co(2-TAPP) in  $\text{CH}_2\text{Cl}_2$  solution and Co(2-TAPP) film, formed from 0.1 M TBAP/ $\text{CH}_2\text{Cl}_2$  solution, with 4131-Å excitation and 6- $\text{cm}^{-1}$  slit widths.

showed no difference between them. Our RR spectra are of the entire film and would not be able to detect small structural modifications of only a few monolayers at the electrode/polymer interface. Since these interface sites are crucial in mediating electron transfer, their modification could result in very different bulk film electrochemical behavior.

**B. Polyaniline-Porphyrins.** Oxidative potential cycling of M(2-TAPP)'s produces adherent electroactive polymers, as also reported by Murray and co-workers.<sup>6,7</sup> The metalloporphyrin units are essentially unaltered in the film, as demonstrated by the resonance Raman spectra of the cobalt complex and its polymer, shown in Figure 5. The excitation wavelength, 413.1 nm, is near resonance with the intense cobalt porphyrin Soret band (412 nm in solution; 434 nm in the film, with the red shift being attributable to excitonic effects as well as coordination of the  $\text{Co}^{\text{II}}$  by N atoms of adjacent TAPP units). The Raman spectra are dominated by porphyrin bands, whose frequencies and relative intensities are essentially the same in the solution and the film. A new band can, however, be discerned at 1547  $\text{cm}^{-1}$ , which may be characteristic of para-substituted polyaniline film, as discussed above. This is one of the strongest polyaniline bands, and its weakness relative to the porphyrin bands reflects the much lower resonance enhancement of polyaniline, whose absorption spectrum is very broad. One other notable difference between solution and film spectra is the replacement of the 1223- and 1257- $\text{cm}^{-1}$  bands of Co(2-TAPP) with a broad band peaking at 1235  $\text{cm}^{-1}$  in the film. The 1223- $\text{cm}^{-1}$  band is assigned<sup>20</sup> to porphyrin-phenyl stretching, and the 1257- $\text{cm}^{-1}$  band, which is not seen in metallo-TAPP's, may be associated with a phenyl mode with substantial phenyl- $\text{NH}_2$  stretching character (observed in aniline at 1278  $\text{cm}^{-1}$ <sup>21</sup>). It is not unexpected that these modes would be perturbed upon polymerization of the aniline groups. The breadth of the band observed in the film is attributable to a variety of interactions with polymer modes, as well as to a distribution of polymerized and unpolymerized aniline groups around the porphyrin ring. Thus,

(20) Burke, J. M.; Kincaid, J. R.; Spiro, T. G. *J. Am. Chem. Soc.* **1979**, *100*, 6077.

(21) Evans, J. C. *Spectrochim. Acta* **1960**, *16*, 248.

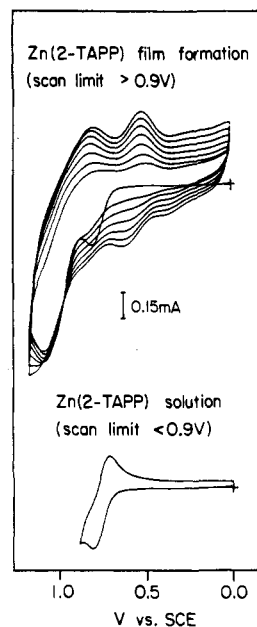


**Figure 6.** Cyclic voltammograms of Zn(2-TAPP) in 0.1 M TBAP/ $\text{CH}_2\text{Cl}_2$  with different positive scan limits. Scan rate was 100 mV/s.

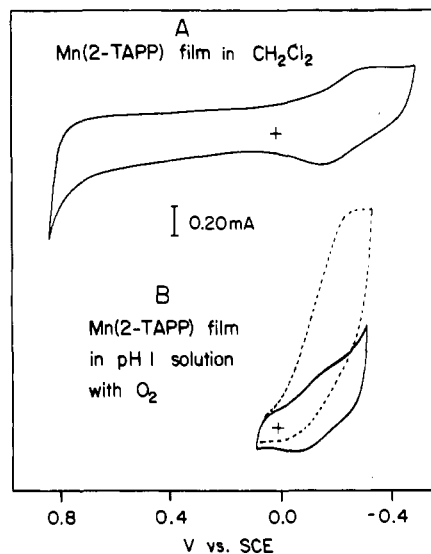


**Figure 7.** Cyclic voltammograms of Mn(2-TAPP) film: (A) in  $\text{CH}_2\text{Cl}_2$ ; (B) in pH 1 solution saturated with  $\text{O}_2$ . Scan rate was 100 mV/s.

the Raman spectra are consistent with the view that the 2-aminophenyl substituents polymerize upon oxidative cycling, just as aniline does, producing an electrode film with intact metalloporphyrin units. While a para-substitution pattern is plausible for the polymerized 2-aminophenyl substituents, the RR spectra cannot rule out alternative patterns, because of the dominance of the porphyrin peaks. Other polymerization pathways are certainly accessible, since Murray and co-workers<sup>7</sup> have shown that 4-TAPP can also electropolymerize. In this case para polymerization is impossible, since the para position is occupied by the porphyrin.

The cyclic voltammograms of these films are complex, due to the superposition of polyaniline and metalloporphyrin redox processes, as noted by Murray and co-workers.<sup>7</sup> The polymerization of Zn(2-TAPP) is instructive with respect to the mechanism of polymerization. Figure 6 shows that Zn(2-TAPP) in methylene chloride gives clean redox waves with  $E_{1/2} = 0.77$  V, characteristic of porphyrin radical cation formation. No polymer is formed on successive cycling provided the potential sweep is not extended beyond 0.9 V. If the sweep is extended further, then rapid polymerization is seen, and the porphyrin radical cation wave is replaced by multiple waves associated with polyaniline. This

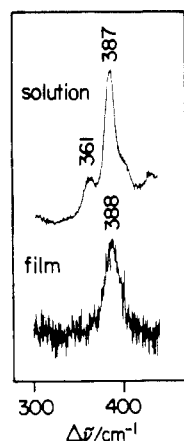


**Figure 8.** Resonance Raman spectra of  $(\text{Fe}(2\text{-TAPP}))_2\text{O}$  solution and  $\text{Fe}(2\text{-TAPP})$  film with 4067-Å laser excitation and 8- $\text{cm}^{-1}$  slit widths.

experiment demonstrates that formation of porphyrin radical cation is insufficient to induce polymerization of the attached aniline groups, in contrast to the situation encountered for protoporphyrin.<sup>3</sup> For zinc protoporphyrin, film formation is observed when the potential is cycled through the radical cation wave and is attributable to cationic vinyl polymerization. In the case of aniline porphyrins, however, the aniline must be oxidized directly to produce polymer.

When  $\text{Mn}(2\text{-TAPP})$  is polymerized, the cyclic voltammogram shows a  $\text{Mn}^{3+/2+}$  redox wave at  $-0.25$  V, negative of the polyaniline redox waves. This wave is shown in Figure 7 for film in contact with methylene chloride. It is also observed when the electrode

film is placed in contact with aqueous electrolyte at pH 4, even though polyaniline itself is nonconductive at this pH.<sup>11</sup> Thus, the metalloporphyrin units in the polyaniline-porphyrin films are electroactive independent of the polyaniline conduction path, as also demonstrated by Murray and co-workers.<sup>7</sup> When air is admitted to the aqueous electrolyte, a large catalytic  $\text{O}_2$  reduction wave is observed at the  $\text{Mn}^{3+/2+}$  potential (Figure 7). Thus, the manganese sites are readily accessible to dissolved  $\text{O}_2$ .

The  $\mu$ -oxo dimer of the iron complex  $(\text{Fe}(2\text{-TAPP}))_2\text{O}$  was electropolymerized by the same procedure, in hopes of producing a film with dimeric porphyrin units. Unfortunately, however, the dimer dissociates on incorporation into the film. Figure 8 shows that the characteristic Fe–O–Fe stretching band at  $361\text{ cm}^{-1}$ <sup>20</sup> is absent in the Raman spectrum of the film. The same phenomenon was encountered with the protoporphyrin  $\mu$ -oxo dimer<sup>3</sup> and was attributed to oxidative dissociation into  $\text{Fe}^{\text{III}}$  and  $\text{Fe}^{\text{IV}}=\text{O}$  units, induced by  $\text{Fe}^{\text{III}}$  coordination in the film. The same mechanism is possible for the 2-TAPP complex.

The metalloprotoporphyrin electrode films were found to be oxidatively unstable in aqueous solution.<sup>4</sup> A single electrode sweep to a potential sufficient to oxidize the films was found to abolish electroactivity, presumably by oxidative processes at the film-electrode interface. We find this to be the case also for metalloaniline-porphyrin films. A single oxidative sweep largely abolishes activity, both for the metalloporphyrin and for the polyaniline redox processes. Again this is presumably due to formation of an insulating layer via oxidation at the film-electrode interface that is catalyzed by the metalloporphyrin units.

**Acknowledgment.** We thank Professor Royce Murray for communicating results of his studies in advance of publication. This work was supported by DOE Grant DE-ACO2-81ER10861.

Contribution from the Departments of Chemistry, Helsinki University of Technology, SF-02150 Espoo, Finland, and University of Joensuu, SF-80100 Joensuu, Finland

## <sup>77</sup>Se NMR Spectroscopic Characterization of Selenium Sulfide Ring Molecules $\text{Se}_n\text{S}_{8-n}$

Risto S. Laitinen\*<sup>1a</sup> and Tapani A. Pakkanen\*<sup>1b</sup>

Received January 9, 1987

<sup>77</sup>Se NMR spectroscopy has been applied to the study of heterocyclic selenium sulfides  $\text{Se}_n\text{S}_{8-n}$  obtained from the molten mixtures of the elements with up to 50 mol % selenium. The assignment of the spectra was based on the combined information from the spectra of the natural-abundance samples and from those of the corresponding <sup>77</sup>Se-enriched samples. The main selenium-containing components in these mixtures were  $\text{SeS}_7$  and 1,2- $\text{Se}_2\text{S}_6$  with smaller amounts of 1,3-, 1,4-, and 1,5-isomers of  $\text{Se}_2\text{S}_6$ , 1,2,3-, 1,2,4-, and 1,2,5-isomers of  $\text{Se}_3\text{S}_5$ , 1,2,3,4-, 1,2,3,5-, 1,2,4,5-, and 1,2,5,6-isomers of  $\text{Se}_4\text{S}_4$ , the 1,2,3-isomer of  $\text{Se}_5\text{S}_3$ , and  $\text{Se}_8$ . In addition,  $\text{Se}_6$ , which is in equilibrium with  $\text{Se}_8$ , could be observed in some samples. The most abundant species within the given isomeric series were those having all selenium atoms adjacent to each other. The trends in the chemical shifts and in the <sup>77</sup>Se-<sup>77</sup>Se coupling constants are presented, and the composition of the phases as a function of the initial melt composition is discussed.

The formation of the eight-membered selenium sulfide ring molecules in the molten mixtures of sulfur and selenium is well established (for two recent reviews, see ref 2). The characterization of the crystalline phases obtained from the melts has, however, turned out to be problematic, because it is not possible to study pure stoichiometric compounds, since different  $\text{Se}_n\text{S}_{8-n}$  species crystallize together forming solid solutions of complex molecular composition.<sup>3</sup> As a result, all crystal structures reported on these phases are disordered with sulfur and selenium randomly distributed over the atomic sites.<sup>5</sup> Therefore, while it can be shown

that the  $\text{Se}_n\text{S}_{8-n}$  molecules indeed are eight-membered crown-shaped rings like  $\text{S}_8$ <sup>6</sup> and  $\text{Se}_8$ ,<sup>7</sup> X-ray crystallography cannot be used for the identification of the molecular species.

Raman spectroscopy is a powerful tool to study heterocyclic selenium sulfides formed in the sulfur-selenium melts.<sup>5c,8</sup> The

- (1) (a) Helsinki University of Technology. (b) University of Joensuu.
- (2) (a) Studel, R.; Laitinen, R. *Top. Curr. Chem.* **1982**, *102*, 177. (b) Gmelin Handbuch der Anorganische Chemie, 8th ed.; Springer Verlag: Berlin Heidelberg, New York, 1984; "Selenium", Suppl. B2, p 280.
- (3) Recent ab initio MO comparison<sup>4</sup> of the electronic structures and properties of the SS, SeS, and SeSe bonds has shown that they are remarkably similar and that the energy change in the transformation of one SS and one SeSe bond into two SeS bonds is small, thereby indicating that the thermal stability of different  $\text{Se}_n\text{S}_{8-n}$  species is similar.
- (4) (a) Laitinen, R.; Pakkanen, T. *THEOCHEM* **1983**, *91*, 337. (b) Laitinen, R.; Pakkanen, T. *THEOCHEM* **1985**, *124*, 293.

- (5) (a) Kawada, I.; Matsumoto, T.; Burzlaff, H.; Hellner, E. *Acta Crystallogr., Sect. A: Cryst. Phys., Diffr., Theor. Gen. Crystallogr.* **1972**, *A28*, S61. (b) Calvo, C.; Gillespie, R. J.; Vekris, J. R.; Ng, H. N. *Acta Crystallogr., Sect. B: Struct. Crystallogr. Cryst. Chem.* **1978**, *B34*, 911. (c) Laitinen, R.; Niinistö, L.; Studel, R. *Acta Chem. Scand.; Ser. A* **1979**, *A33*, 737.
- (6) (a) Coppens, P.; Yang, Y. W.; Blessing, R. H.; Cooper, W. F.; Larsen, F. K. *J. Am. Chem. Soc.* **1977**, *99*, 760. (b) Templeton, L. K.; Templeton, D. H.; Zalkin, A. *Inorg. Chem.* **1976**, *15*, 1999. (c) Watanabe, Y. *Acta Crystallogr., Sect. B: Struct. Crystallogr. Cryst. Chem.* **1974**, *B30*, 1396.
- (7) (a) Cherin, P.; Unger, P. *Acta Crystallogr., Sect. B: Struct. Crystallogr. Cryst. Chem.* **1972**, *B28*, 313. (b) Marsh, R. E.; Pauling, L.; McCullough, J. D. *Acta Crystallogr.* **1953**, *6*, 71. (c) Foss, O.; Janickis, V. *J. Chem. Soc., Dalton Trans.* **1980**, 624.
- (8) (a) Ward, A. T. *J. Phys. Chem.* **1968**, *72*, 4133. (b) Eysel, H. H.; Sunder, S. *Inorg. Chem.* **1979**, *18*, 2626. (c) Laitinen, R.; Studel, R. *J. Mol. Struct.* **1980**, *68*, 19.